

Signature of the Gravity Wave Phase Shift in a Cold Quark Star with a Nonconvex Multicomponent van der Waals Equation of State

Keith Andrew¹, Eric Steinfelds², Kristopher Andrew³

¹Department of Physics and Astronomy, Western Kentucky University
Bowling Green, KY 42101 USA

²Department of Computational and Physical Sciences, Carroll University,
Waukesha, WI 53186 USA

³Department of Science, Schlarman Academy,
Danville, IL 61832 USA

Abstract

We investigate nonclassical BZT rarefaction shocks and the QCD phase transition in the dense core of a cold quark star in beta equilibrium subject to the multicomponent van der Waals (MvdW) equation of state (EoS) as a model of internal structure. When this system is expressed in terms of multiple components it can be used to explore the impact of a phase transition from a hadronic state to a quark plasma state with a complex clustering structure. The clustering can take the form of colored diquarks or triquarks and bound colorless meson, baryon, or hyperon states at the phase transition boundary. The resulting multicomponent EoS system is nonconvex which can give rise to nonclassical Bethe-Zel'dovich-Thompson (BZT) phase changing shock waves. Using the BZT shock wave condition we find constraints on the quark density and examine how this changes the compactness and tidal deformability of the compact core. These results are then combined with the TOV equations to find changes in the mass - radius relationship. These states are compared to recent astrophysical high mass neutron star systems which may provide evidence for a core that has undergone a quark-gluon phase transition such as PSR 0943+10 or GW 190814.

Keywords: nonconvex; van der Waals; BZT; shock wave; gravity wave

I. Introduction

The study of the interacting dynamics of cold quark matter in beta equilibrium to understand a portion of the QCD phase diagram to describe the existence of compact stellar objects has grown considerably with the discovery of anomalous events such as the stellar remnant from the energetic hypernova 2006gy [1]. This event, caused by the sudden collapse of a high mass star, gave rise to final state mass and radius values that can differ from standard compact stellar core models. The ongoing observational datasets now include the anomalous X-ray pulsar [2] RX J1856 [3,4] and pulsars such as PSR 0943+10 [5], PSR B1828-11 [6], PSR J0751+1807 [7], PSR B1642-03, PSR J1614-2230 and PSR J0348-0432 along with potential GRB candidates GRB 050709 [8] and GRB170817A [9, 10], kilonovae -GW 190425 [11,12] and magnetar candidates such as 1E 2259+ 586 [13, 14], and gravity wave events [15, 16] where masses, radii, dual luminosity peaks and cooling rates do not always give extraordinary fits to conventional models based upon degenerate neutron matter. Improvements in the observational data has resulted in

more detailed models to help understand the varied mechanisms at play in dense QCD matter beyond the nuclear saturation limit of $\sim 0.16 \text{ fm}^{-3}$. New models [17] are gaining support from the observations of the Quark Gluon Plasma, QGP, demonstrating the existence of a high temperature, low chemical potential state of unconfined quarks as seen at SPS [18], LHC [19] and RHIC [20,21] laboratories. In recent years the QGP data has expanded to include the determination of relativistic QCD based transport coefficients [22] and measurements of the overall bulk viscosity for free quark matter. [23,24] Observations of X-ray, γ - ray and quasi periodic objects such as SAS J1808.4 -3658 which has a 2.49 ms period [25] have been used to understand how the environment [22] and the ambient mass density impacts fundamental QCD parameters and potentials [26]. Various EOS have been used linking the strong coupling constant and quark masses to the local density function using the real time formalism and the Dyson-Schwinger gap equation at finite temperature [27]. In this way high density compact cores can be used to give the density dependent strong coupling that can be expressed in a way that is suitable for EOS and phase transition analysis [28] with high chemical potentials and lower temperatures. The high resolution data from the NICER satellite has extended and constrained the EoS modeling with X-ray spectra [29] for masses and radii.[30]

For a collapsing star in beta equilibrium the overall charge, density, and chemical potentials are constrained by overall charge neutrality for particle number density n_j , mass density ρ_f and electric charge q_j for particle type j or flavor f : $\sum q_f n_f = q_e n_e$ and $\rho_B = \rho_u + \rho_d + \rho_s$ and three light quark flavor weak interaction equilibrium from quark interactions $d \leftrightarrow u + e^- + \bar{\nu}_e$, $s \leftrightarrow u + e^- + \bar{\nu}_e$, $s + u \leftrightarrow d + u$ constraining the chemical potentials where the neutrinos and antineutrinos exit the core on a short time scale compared to the core formation process effectively causing their chemical potentials to vanish resulting in $\mu^d = \mu^u + \mu^e$, $\mu^s = \mu^u$. The classical pressure is related to the chemical potential from $P = -\partial U / \partial V = n^2 \partial(\epsilon/n) / \partial n = n\mu - \epsilon$ where the chemical potential is $\mu = \partial \epsilon / \partial n$. For the massless quark case this gives a direct comparison to the MIT bag model³¹ with bag constant B where $3P = (\epsilon - 4B) = \epsilon - 4(3\mu^4/4\pi)$ linking [32] the vacuum pressure bag constant to the quark chemical potentials which are energy dependent. Several compact core models have focused on modified EOS for various states of dense matter in the QCD ground state of Color Flavor Locked (CFL) dense matter [33, 34] with 2-d and 3-d color superconductivity [35,36,37] and in the Nambu-Jona-Lasinio (NJL) model [38]. Many models admit to a comparison to versions of the generalized MIT Bag model [39] approach and include QCD mean field approximations [40,41] quarkyonic matter [42 43] along with computationally intensive numerical lattice approaches that are being improved to accommodate finite temperature chemical potentials. [44] Refined models include crustal effects [45], deformations [46], layering [47], cooling rates [48], strange quark cores, finite temperature boson stars [49] and kaon condensation [50,51] superconducting color vector potential effects [52,53], phase transitions, and different crystalline cores [54,55,56]. In many cases these EoS are everywhere convex, however, there are a number of cases where the pressure and density are so extreme that the EoS will become nonconvex. In the case of relativistic hydrodynamics [57, 58] the energy momentum tensor [59] has a term proportional to the enthalpy which includes a factor of $P/\rho c^2$, or a factor of $4B/\rho c^2$ for the MIT Bag model, which is normally quite small. At high pressures this term makes a larger contribution and, when asymptotic freedom is considered leading to free fast-moving particles, this term can be significant. At first this correction will drive the system closer to a stable point, but for high core pressures it can continue to push the system into an unstable region of shock waves that will alter the phase transition. Such phase transitions, occurring in the nonconvex region of the EoS, have

been studied by Bethe [60], Zel'dovich [61] and Thompson [62] and these fluids are now known as BZT fluids. They developed a fundamental derivative test to identify when a fluid could develop BZT behavior. This has been used in the study of neutron stars by Aloy et. al. [63] where they develop a method for measuring the BZT signature in gravitational waveforms. [64, 65] The BZT phase transitions can have regions of spinodal decomposition leading to the formation of quark clusters and diquark states from the color states for color group $SU(3)_C \rightarrow 3 \otimes 3 = \bar{3} + 6$, where the antisymmetric color factor is attractive, $C(F) < 0$, and the symmetric is a weaker repulsive force, $C(F) > 0$. Here we will apply the multicomponent van der Waals model to investigate the hadron to quark phase transition in a compact stellar core in beta equilibrium with a BZT region identified by the fundamental derivative test. As noted by Gosh [66] and Vovchenko [67] where they investigate the nuclear models and van der Waals [68] correspondence from the resonance hadron gas mode to lattice QCD, this model provides an analytical model with a critical point, it can model composite quark clusters as color singlets or net color carriers [69], it includes a phase transition, it can support shock wave behavior, it includes an excluded volume limit [70, 71], the parameters are selected in alignment with lattice models, and can include both a repulsive or attractive strong force limit using color factor couplings depending upon the color group representation of $SU(3)_C$. As such several authors have used the van der Waals (vdW) equation [72, 73, 74, 75, 76, 77] of state (EoS) provides a useful analytical framework to describe the complex interactions within a hadronic medium under extreme conditions [78, 79, 80, 81, 82, 83].

However, the MvdW EoS phase transition zone admits a nonconvex region that allows for BZT shock waves to form. When the BZT fundamental derivative becomes negative the conditions for nonclassical anomalous wave formation exist. The BZT compression can lead to a rapid dispersion and an undefined speed of sound. In this case the nonconvex MvdW EoS [84, 85] can be used to describe the BZT phase transition as being spinodal. Due to the nonclassical behavior of shock waves in this region spinodal clumping of mixed phases is expected to occur [86]. Isreal has recently developed a relativistic generalization of these BZT fundamental derivative results opening a new regime to explore. As a result, the compression can be purely classical, or a nonclassical BZT type, or a nonclassical relativistic BZT type. This nonlinear wave propagation and dispersion leads to a shift or reduction or phase shift in gravity wave production whose signature can be searched for using LIGO, VIRGO, KAGRA, Einstein Telescope or LISA data or simulations. In general shock waves in a BZT hadron fluid with a negative fundamental derivative could contribute to a QCD phase transition by creating nonclassical localized high density regions conducive to quark formation facilitated by quark nuggets or noncolor singlet quark clusters. This could result in a broader and more easily sustained phase transition to a stellar quark core leaving a unique gravity wave or luminosity signature that can be partially modeled by a MvdW EoS. This paper is organized as follows: the next section introduces the multicomponent van der Waals partition function and the various thermodynamic functions used to calculate the fundamental derivative and its relativistic correction with a special focus on the BZT regions, the following section models the gravitational wave signature of the BZT zone through the tidal deformability modeled from solutions to the TOV equation with the MvdW EoS, finally these are compared to the sensitivity range needed for detection, finally ending with a concluding section. We use units where $G=c=k=1$ and the lower-case letter for thermodynamic variables that are specific densities per volume.

II vdW Partition function and Fundamental Derivative

Here we calculate the thermodynamic quantities needed to derive the BZT fundamental derivative for the MvdW EoS. Starting with the partition function we will calculate the internal energy and enthalpy for our system. The MvdW partition function for a total of N_c different components, where each component species can have N_i particles, each with a van der Waals volume of b_k , with a mean field interaction coupling strength given by a_{ij} , in a total volume V , at temperature T , is given by

$$Z_{vdw}(N_i, V, T) = \prod_{i=1}^{N_c} \frac{1}{N_i!} \left(\frac{V - \sum_{j=1}^{N_c} N_j b_j}{\Lambda_i^3} \right)^{N_i} \exp\left(\frac{N_i}{VkT} \sum_{j=1}^{N_c} a_{ij} N_j \right) \quad (1)$$

where the i^{th} particle species has a thermal de Broglie wavelength given by

$$\Lambda_i = \sqrt{\frac{1}{2\pi m_i T}} \quad (2)$$

For our applications the interaction couplings will obey a mixing rule where a_{ij} is symmetric and can be considered as the product of the individual particle couplings a_i where we use the interaction parameter k_{ij} expressed as

$$a_{ij} = \sqrt{a_i a_j} (1 - k_{ij}) = a_{ji} \quad (3)$$

The values of the a_{ij} terms reflect the different color factor interactions and can represent attractive or repulsive interactions. The pressure can be expressed in terms of particle species number N_i or number volume density

$$p = T \left(\frac{\partial \ln Z}{\partial V} \right)_{N,T} = T \sum_{i=1}^{N_c} \left[\frac{N_i}{V - \sum_{j=1}^{N_c} N_j b_j} - \frac{N_i}{V^2 T} \sum_{j=1}^{N_c} N_j a_{ij} \right] = \frac{\sum_{i=1}^{N_c} n_i T}{\left(1 - \sum_{j=1}^{N_c} n_j b_j \right)} - \sum_{i=1}^{N_c} \sum_{j=1}^{N_c} n_i n_j a_{ij} \quad (4)$$

The internal energy is given by

$$U = kT^2 \left(\frac{\partial \ln Z}{\partial T} \right)_{N,V} = T \sum_{j=1}^{N_c} N_j - \frac{1}{V} \sum_{i=1}^{N_c} \sum_{j=1}^{N_c} a_{ij} N_i N_j \quad (5)$$

and the entropy per particle is given by

$$S_p = S_0 + \sum_{i=1}^{N_c} \frac{N_i}{N} \ln \left(\frac{V_p - b_{mix}}{\Lambda_i^3} \right) - \sum_{i=1}^{N_c} \frac{N_i}{N} \ln \left(\frac{N_i}{N} \right) \quad (6)$$

Which will be used to express the pressure and the classical enthalpy in terms of entropy and volume to evaluate along an entropic curve, and the enthalpy volume density is

$$h = u + pV = \frac{3}{2} \frac{N}{V} T - 2 \sum_{i=1}^{N_c} \sum_{j=1}^{N_c} a_{ij} \frac{N_i}{V} \frac{N_j}{V} + \frac{T(N/V)}{1 - \sum_{j=1}^{N_c} \frac{N_j}{V} b_j} \quad (7)$$

We simplify these expressions by introducing a scale factor based on the total number of particles, N , for each particle species number fraction x_i , the total van der Waals mixture volume of the particles, b_{mix} , and mixture interaction couplings, a_{mix} ,

$$N = \sum_{k=1}^{N_c} N_k \quad x_i = \frac{N_i}{N} \quad V_p = \frac{V}{N} \quad b_{mix} = \sum_{k=1}^{N_c} x_k b_k \quad a_{mix} = \sum_{j=1}^{N_c} \sum_{k=1}^{N_c} x_j x_k a_{jk} \quad n_i = \frac{N_i}{V} \quad \delta = \frac{R}{c_V} \quad (8)$$

where the specific heat is related to the number of degrees of freedom for the i^{th} particle species. Using these variables the multicomponent van der Waals EoS and enthalpy become

$$p(V, T) = \frac{RT}{V_p - b_{mix}} - \frac{a_{mix}}{V_p^2} \quad e = \frac{RT}{\delta} - \frac{a_{mix}}{V_p} + e_0 \quad s = R \ln \left[(V_p - b_{mix}) \left(e + \frac{a_{mix}}{V_p} \right)^{\frac{1}{\delta}} \right] + s_0 \quad (9)$$

Changing variables to entropy and volume we have

$$P(T, V) \rightarrow P(s, V_p) = \frac{\delta \exp \left[\frac{\delta(s - s_0)}{R} \right]}{(V_p - b_{mix})^{\delta+1}} - \frac{a_{mix}}{V_p^2} \quad (10)$$

The first classical fundamental derivative is

$$G_{cl} = -\frac{1}{2} V \frac{\left(\frac{\partial^2 P}{\partial V^2} \right)_s}{\left(\frac{\partial P}{\partial V} \right)_s} \quad (11)$$

Where the multicomponent van der Waals classical BZT first fundamental derivative along an isentrope is

$$G_c = \frac{(\delta+1)(\delta+2)V_p^5 \left(P + a_{mix}/V_p^2 \right) - 6a_{mix}V_p \left(V_p - b_{mix} \right)^2}{2V_p^4 (\delta+1) \left(V_p - b_{mix} \right) \left(P + a_{mix}/V_p^2 \right) - 4a_{mix}}. \quad (12)$$

This gives the standard value in the limit of a single component and, when taking the ideal gas limit, we have a value of $G_{cl} = 1 + \delta/2$ in agreement with the convex ideal gas law, in the limit of a single component we get the standard vdW value, in the limit of no excluded volume we get the simplified ideal gas volume dependence and in the limit of no interactions with the excluded volume we get the interacting gas expression. The locus of points (P, V) for $G=0$ corresponding to the boundary between the classical and nonclassical regimes is found by solving for the pressure to get

$$P(G=0) = \frac{a_{mix}}{V_p^2} \left[\frac{6}{(\delta+1)(\delta+2)} \left(1 - \frac{b_{mix}}{V_p} \right)^2 - 1 \right] = n^2 a_{mix} \left[\frac{6(1 - nb_{mix})^2}{(\delta+1)(\delta+2)} - 1 \right]. \quad (13)$$

The relativistic fundamental derivative is defined from the energy momentum tensor enthalpy for fermions using the Fermi-Dirac distribution function given by

$$\begin{aligned} T^{\mu\nu} &= nh u^\mu u^\nu + p g^{\mu\nu} \\ nh &= \frac{g}{(2\pi)^3} \int \sqrt{p^2 + m^2} f(p) d^3 p - \sum_{i,j} a_{ij} n_i n_j + \frac{\sum_i n_i T}{1 - \sum_i b_i n_i} - \sum_{i,j} a_{ij} n_i n_j \\ nh &= \frac{g}{8\pi^2} \left[p_F \sqrt{p_F^2 + m^2} (2p_F^2 + m^2) - m^4 \ln \left(\frac{p_F + \sqrt{p_F^2 + m^2}}{m} \right) \right] - \sum_{i,j} a_{ij} n_i n_j + P \\ c_{cl}^2 &= \left(\frac{\partial P}{\partial n} \right)_s. \end{aligned} \quad (14)$$

For a cold star in beta equilibrium composed of nondegenerate fermions along an isentrope this becomes

$$\begin{aligned} nh &= 2\pi^{2/3} n^{4/3} - 2 \sum_{i,j} a_{ij} n_i n_j & G_{sr} &= -\frac{3}{2} c_{sr}^2 = -\frac{3}{2h} \left(\frac{\partial P}{\partial n} \right)_s \\ G_{Total} &= G_{cl} + G_{sr} = G_{cl} - \frac{3c_{cl}^2}{2h} = G_{cl} - \frac{6(\delta+1) \left(P + n^2 a_{mix} \right) + 12n^2 a_{mix}}{2(1 - nb_{mix}) \left(\pi^{2/3} n^{4/3} - n^2 a_{mix} \right)}. \end{aligned} \quad (15)$$

Eq. (15) can provide better treatment for the high density behavior found in compact stellar cores, for equilibrated neutron stars well below the Fermi energy the temperature terms are very small and can be neglected for modeling, and the multicomponent nature of the MvdW EoS will allow us to explore the impact of having several particle species in the core where both attractive and repulsive interacting terms that can be tested using the interaction potential terms in the a_{ij} and k_{ij} factors. The relativistic term to the fundamental derivative value can shift a region that was an otherwise convex classical region into a new nonconvex BZT spinodal decomposition mixed fluid zone thereby altering the phase change dynamics of the core. The clumping that develops from this phase change leads to increased nonclassical shocks and rarefactions whose signature can be apparent in the shift in the phase peak of the gravity wave spectrum. For positive classical fundamental derivatives, the relativistic correction can lower the value of the fundamental derivative closer to zero thereby smoothing out fluctuations that could give rise to instabilities, as long as it does not become negative. In Fig. (1) we plot several special cases of the BZT fundamental derivative and the relativistic correction for the multicomponent van der Waals EoS where the negative regions correspond to the rarefaction shock wave zones.

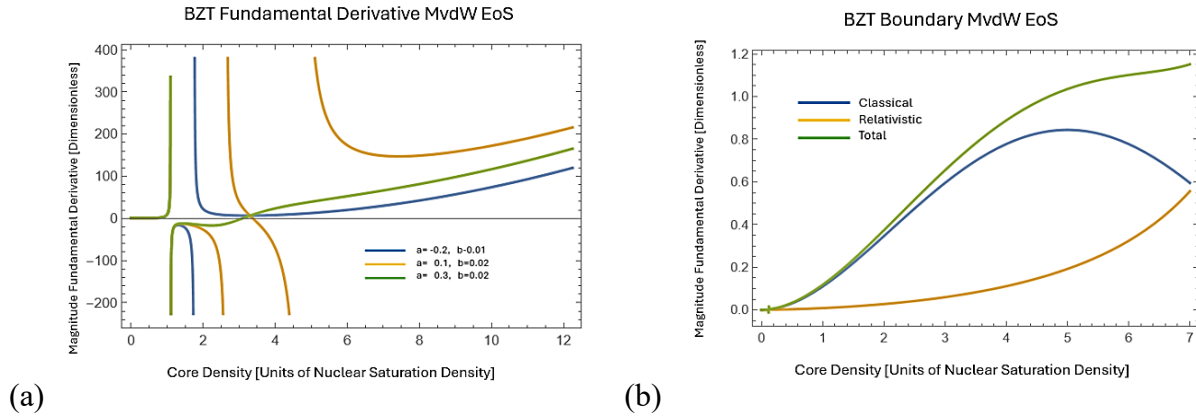


Fig. 1 (a) The first fundamental derivative for the multicomponent van der Waals equation of state showing positive and negative BZT regions for different strengths, densities, and relativistic corrections. (b) The fundamental derivative boundary between the BZT zone and classical zone and the relativistic contribution to the total.

To numerically evaluate Eqs.(12)-(15) we select the constituents to be point particles with three degrees of freedom, there are no degeneracies between states, and all densities are in units of nuclear saturation density.

III Peak Gravity Wave Shift Signature of BZT Shocks and Chirps

The spinodal decomposition during the phase change results in anomalous dispersion and shock wave formation that will alter the gravity wave signature of a wave producing event with a BZT compact stellar core. The gravitational wave amplitude varies as $h(f) \sim (M_{\text{ch}})^{5/3} f^{-7/6} / D$, for chirp mass M_{ch} defined in Eq.(18), frequency and distance D , these changes are currently beyond

detectability, however the phase shift for a BZT EoS is closer to the range of detectability so we will analyze it more closely. We determine the mass and radius values from the TOV equations

$$\frac{dP}{dr} = \frac{Gm\rho\left(1 + \frac{P}{\rho}\right)\left(1 + 4\pi r^3 \frac{P}{m}\right)}{r^2\left(1 - \frac{2m}{r}\right)}$$

$$\frac{dm}{dr} = 4\pi r^2 \rho$$
(16)

Which we solve numerically for the MvdW EoS for different values of the parameters a_{mix} , b_{mix} , k_{ij} , and N_c with plots presented in Fig.(2). The stability can be examined using the EoS adiabatic index test:

$$\Gamma = \frac{\partial \ln P}{\partial \ln \rho} > \frac{4}{3}$$

$$\frac{\partial \ln P}{\partial \ln \rho} = \frac{(1 - N_c n b) \left[N_c T (1 + N_c n b) - 2 N_c^2 a n (1 - N_c n b)^2 \right]}{(N_c T - a N_c^2 (1 - N_c n b))} > \frac{4}{3}$$
(17)

Eq.(17) is used to constrain the values of a , b , and n to be in a range that leads to a stable configuration. Expressed in terms of the number of components N_c , the particle number density n , the interaction potential a , the excluded volume b , which behaves like a repulsion under extreme compression, and the temperature T . Eq.(17) is plotted in Fig. 2 for several different models where the critical stable adiabatic index line is the red dotted line. The system becomes more stable as a is decreased and b is increased. Increasing a for higher densities mimics the asymptotic freedom effects seen in short range QCD. Models with $a > 0$ and $b > 0$ exhibit monotonic increases as the density increases.

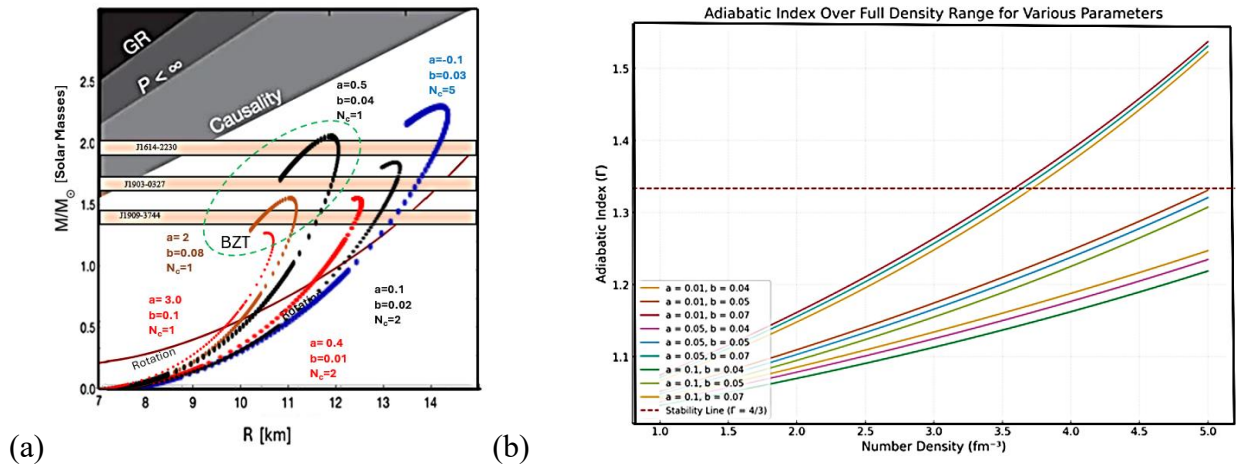


Fig. 2 (a) Solutions to the TOV equations exhibiting maximum mass and radii for MvdW EoS with different components, a_{mix} and b_{mix} showing the steady shift into the BZT zone for fewer components, smaller b_{mix} , and larger positive a_{mix} values. (b) Increasing the adiabatic stability index for various models displaying a trend towards the stability line with increasing density.

Where in Fig. (2) we show numerical solutions exhibiting the mass and radius limits. We also show three candidate pulsars: J1614 -223-, J1903-0327 and J1909-3744 which have estimated mass near 1.5 and 2.0 solar masses. The waveform shift is influenced by the tidal deformability, Λ , the compactness C , and the second Love number k_2 , where compactness values are determined from the TOV equations for the MvdW EoS for different particle content, and for a merging binary system the system compactness scales with the chirp mass, the merger tidal deformability depends on the individual masses and tidal deformability and the gravity wave phase shift can be expressed in terms of the chirp mass and merger deformability as

$$C_j = \frac{M_j}{R_j}, \quad \Lambda_j = \frac{2}{3} k_2 C_j^{-5} \quad M_{ch} = \frac{(M_1 M_2)^{3/5}}{(M_1 + M_2)^{1/5}} \quad k_{2_{MvdW}} = \frac{8}{5} \left[\frac{C_j^5 (1 - 2C_j)^2}{1 + a_{\text{mix}} C_j + b_{\text{mix}} C_j^2} \right]$$

$$\tilde{\Lambda}_{merger} = \frac{16 (M_1 + 12M_2) M_1^4 \Lambda_1 + (M_2 + 12M_1) M_2^4 \Lambda_2}{(M_1 + M_2)^5}$$

$$\Delta\Psi = \frac{3}{128} (\pi M_{ch} f)^{-5/3} \tilde{\Lambda}_{merger}$$
(18)

The compactness and tidal deformability depend on the TOV masses and radii found for each EoS allowing for a comparison between the various models where several cases are presented in Fig. (3). The Love number decreases with density and the tidal deformability decreases with compactness. For the MvdW EoS the stronger interactions for a > 0 and smaller number of components gives a higher compactness and stiffness resulting in less deformability while a lower excluded volume, $b \ll 1$, leads to a greater tidal deformability.

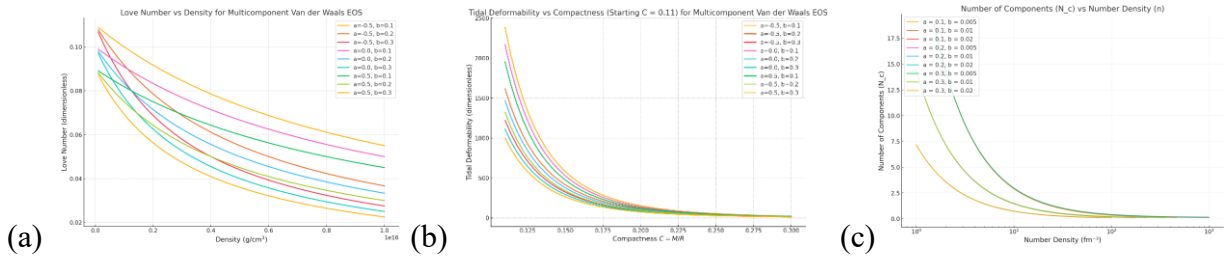


Fig. 3 (a) Comparison of second Love numbers and (b) Tidal deformability for neutron stars and quark stars using the multicomponent van der Waals EoS. (c) Number of Components vs. Number Density using the multicomponent van der Waals EoS. The number of components effectively alters the value of the interaction term a_j and tends to soften the EoS as the number of components increases.

Typically, the quark star has a higher compactness due to the increased density leading to a lower tidal deformability when compared to a neutron star prior to the phase transition. The range of values is presented below in Table 1.

Parameter	Neutron Stars	Quark Stars
Compactness (C)	0.15 – 0.25	0.2 – 0.35
Love Number (k_2)	0.05 – 0.15	0.01 – 0.05
Tidal Deformability (Λ)	200 – 1000	10 – 100
Chirp Mass (\mathcal{M})	1.18 – 1.20 M_\odot	0.96 – 1.15 M_\odot
Merger Tidal Deformability ($\tilde{\Lambda}$)	70 – 720	10 – 100

Table 1. Here are the comparison values for a neutron star and quark star for compactness, Love number, tidal deformability, chirp mass and the merger tidal deformability.

The wave phase shift depends upon the EoS and the chirp mass, for the BZT region we plot this change in Fig. (4). Overall, the stiffer EoS gives a smaller shift due to reduced tidal effects with high compactness which is most pronounced at low frequencies. In the MvdW EoS this corresponds to the fewest components with the largest attractive force, $a > 0$, and smallest excluded volumes, $b \ll 1$. Likewise, higher chirp masses lead to greater compactness and smaller phase shifts. Each model EoS gives a phase shift in accordance with the associated stiffness of the model.

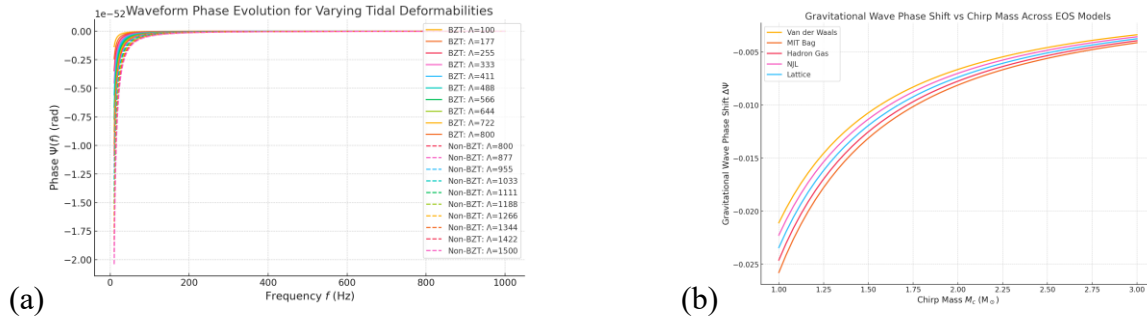


Fig. 4 (a) The BZT gravitational wave phase shift as a function of frequency for different tidal deformability for the van der Waals EoS in the convex and BZT state with positive and negative a values indicating attractive and repulsive interactions. (b) A range of modified comparison models with added BZT zones: Modified MIT Bag Model, Modified Hadron Gas Model, Modified NJL Model and a Lattice Model to compare directly to the MvdW EoS.

The BZT regions reduce the energy going into the compression regions thereby altering the coexistence energy distribution with anomalous dispersion and resulting in the peak energy to be delayed and frequencies to be shifted to lower values.

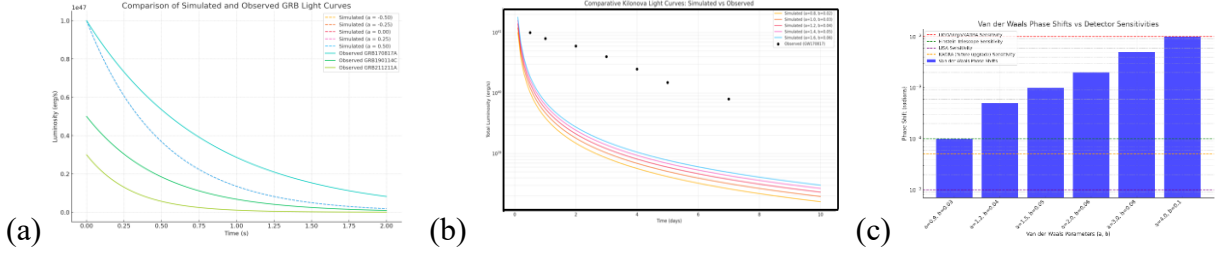


Fig. 5 (a) Simulated total luminosity for a GRB light curve with attractive and repulsive interaction strengths in the multicomponent van der Waals EoS for a GRB event compared to three observed GRBs. (b) Comparison to kilonova event GW 170817 for $0.8 < a \text{ MeV fm}^3 < 1.2$ and $0.02 < b \text{ fm}^3 < 0.06$. (c) A comparison of the maximum vdW BZT phase shift frequency dependence to the current and estimated sensitivities for the LIGO, VIRGO, KAGRA, Einstein Telescope and LISA facilities.

For comparison we use modified BZT versions of the following models: the MIT Bag model, the Hadron Gas model, the NJL model and a Lattice Model. To introduce BZT regions we include interaction terms: in the MIT model we use the standard extension of a van der Waals like interaction with a bag constant [87, 88], in the Hadron Gas Model the interaction term includes a field that repels and attracts [89], the NJL model has a BZT region for the chiral symmetry breaking that is a part of the model [90, 91], the lattice model uses a pQCD term that drives the pressure derivatives negative [92, 93]. While it is possible to produce BZT regions in each model the impact varies in extent and significance. In the modified MIT Bag model, the BZT region exhibits a strong dependence on the magnitude of the interaction parameter, in the Hadron Gas model the BZT region only appears near hadronic saturation density and is highly localized, in the NJL model BZT effects are prominent and impactful in the chiral transition region, in lattice models BZT regions only occur near the critical point at high chemical potentials. In Fig. (5) we present estimates for the gravity wave phase shift for each model as a function of the associated chirp mass. The overall trend is similar for each BZT region with a merging of all values for high chirp mass. For low chirp mass the single component van der Waals has the largest shift while the modified MIT bag model has the largest shift. Fig. (5) shows a comparison of the MvdW EoS luminosity curve to three GRB events: GRB 170817A, GRB 190114C, GRB 211211A and to the kilonova event GW 170817. In all cases the MvdW model has too steep a decay even for large values of a and b which do not match the required asymptotic freedom and phase change constraints.

Gravitational Wave Detector Comparison and Phase Shift Sensitivity

	Detector	Frequency Range (Hz)	Sensitivity (Strain)	SNR Threshold	Application	Phase Shift Sensitivity
1	LIGO	10-1000	$\sim 10^{-23}$	~ 8	Binary mergers, neutron stars, black holes	10^{-2}
2	Virgo	10-1000	$\sim 10^{-23}$	~ 8	Binary mergers, neutron stars, black holes	10^{-2}
3	LISA	0.01-1	$\sim 10^{-21}$	~ 1	Supermassive black holes, early universe	10^{-5}
4	Einstein Telescope	1-1000	$\sim 10^{-24}$	~ 5	Binary mergers, cosmological signals	10^{-4}
5	KAGRA	10-1000	$\sim 10^{-23}$	~ 8	Binary mergers, neutron stars, black holes	10^{-3}

Table 2. Here we collect the typical response characteristics of detectors that can find evidence for the predicted phase shift, the KAGRA data is for the current upgrade.

Comparing the values from Table 2 [94] with the phase shifts expected in Fig. (5). The LIGO [95]-VIRGO [96]-KAGRA [97] detectors have phase shift sensitivities ~ 0.02 radians which would require MvdW parameters of $a > 4 \text{ MeV fm}^3$ and $b < 0.01 \text{ fm}^3$. These values do not result in a likely scenario at the required high densities given that QCD forces exhibit asymptotic freedom at short distances. The upgraded Einstein telescope [98] requires $a \sim 1.2 \text{ MeV fm}^3$ and $b \sim 0.04 \text{ fm}^3$ to produce observable phase shifts, these values are in the range expected during a BZT phase transition and could lead to a measurable result. The future LISA [99] detector should be in this range and could constrain the values used for the MvdW EoS.

IV Conclusions

We have used the nonconvex MvdW EoS to investigate the impact of the nonconvex region on the phase shift of a gravitational wave event and a GRB luminosity model to search for a detectable BZT EoS signal. In typical neutron matter classical compressive shock waves tend to dissipate energy by heating the fluid, such action might disrupt and prevent a full QCD phase transition unless the conditions are extreme. When the fundamental derivative is negative the compression waves will not steepen into localized shocks but rather the waves tend to disperse and rarify upon compression producing QCD cavitation, this nonlinear anomalous shock propagation alters the phase transformation and can produce unstable metastable states very sensitive to the thermodynamic state, especially near any critical points. This behavior creates unique local variations in pressure and density which alter the conditions needed for a phase transition. This results in a coexistence region with pronounced clumping with quark clusters, nuggets and diquark states, which can be metastable, and alternate with volumes of quark gluon plasma states with deconfined quarks, this behavior leads to potentially unusual and spatially

complex phase behaviors not observed in fluid with a positive fundamental derivative. However, in a BZT neutron fluid the nonclassical shock dynamics will mean that localized energy and density fluctuations could sustain a phase transition at lower average energy levels than in standard neutron matter. This could result in a relatively low energy path to quark matter formation compared to the direct collapse model assumed for many cases. In our study we have used the TOV equations for a spherical mass with no magnetic field, and there is no rotation, these are modifications we are currently exploring. In addition, the MvdW EoS has a natural limit to a polytropic star which provides a canonical system to investigate in parallel with the MvdW EoS. There is also extensive work on introducing the Maxwell construction to remove the nonconvex region while having the speed of sound vanish, due to no pressure gradients, while others favor the Gibbs construction to maintain chemical potentials, both methods change the dynamics of the coexistence phase. In a similar way one can also use an infrared regulator in the interaction term to reduce or remove the nonconvex region. We also are implementing a density dependent interparticle force to explore a change in the van der Waals luminosity function to better match a typical GRB curve. The BZT rarefaction shocks will also modify the thermal conductivity and heat transport, thereby affecting the star's cooling behavior. The shocks will impact neutrino production in direct Urca process: $n \rightarrow p + e^- + \bar{\nu}_e$ $p + e^- \rightarrow n + \nu_e$ and the modified Urca process: $n + n \rightarrow p + n + e^- + \bar{\nu}_e$ $p + n + e^- \rightarrow n + n + \nu_e$ where the edge density gradients should enhance neutrino production and alter neutrino emissivity impacting potential kaon condensates. Rarefaction shocks would also reduce thermal insulation and alter the heat transport to the surface causing a higher cooling rate and a lower surface temperature, perhaps similar to what is observed at Cas A [100].

Here we have used the MvdW EoS to examine the fundamental derivative indicating the onset of nonconvex behavior and looked at how this would induce a shift in the phase of a gravity wave producing event. We then examined if this could produce a measurable signature indicating the presence of internal BZT structure. We found that the formation of unusual nonclassical shock waves in a BZT hadron fluid with a negative fundamental derivative could contribute to a QCD phase transition by creating localized, high-density regions, conducive to quark gluon plasma formation along with adjacent BZT low density rarefaction regions providing a possible means for a sustained novel phase transition. This unique behavior could facilitate the formation of quark nuggets or quark clusters, which, under the right conditions, could lead to a broader phase transition, potentially transforming the stellar core into a quark star without the need for ever higher pressures. As such the unusual BZT properties of a hadron fluid could provide a unique mechanism by which extreme astrophysical conditions might initiate and sustain a phase change to quark matter. The formation of such an object could leave a signature in the gravity wave phase shift that could best be observed in a future gravity wave detector such as LISA or the Einstein Telescope.

Author Contributions: Formal Analysis: KA, ES, KAA; Methodology: KA, ES, KAA, Investigation: KA, ES, KAA; Formal Analysis, Numerical Solutions and Visualization: KA, ES,

KAA; Writing original draft: KA; Writing review and editing: KA, ES, KAA. All authors have read and agreed to the published version of the manuscript

Funding: This research received no external funding.

Data Availability Statement: Not applicable.

Acknowledgments: The authors wish to thank Western Kentucky University and Schlarman Academy for their kind support throughout the work on this project, all plots and numerical solutions were generated in Mathematica.

Conflicts of Interest: The authors declare no conflict of interest.

-
1. Smith, Nathan, Weidong Li, Ryan J. Foley, J. Craig Wheeler, David Pooley, Ryan Chornock, Alexei V. Filippenko et al. "SN 2006gy: discovery of the most luminous supernova ever recorded, powered by the death of an extremely massive star like η Carinae." *The Astrophysical Journal* 666, no. 2 (2007): 1116.
 2. Xu, Renxin. "Strange quark stars: observations and speculations." *Journal of Physics G: Nuclear and Particle Physics* 36, no. 6 (2009): 064010.
 3. Burwitz, Vadim, F. Haberl, R. Neuhäuser, P. Predehl, J. Trümper, and V. E. Zavlin. "The thermal radiation of the isolated neutron star RX J1856. 5–3754 observed with Chandra and XMM-Newton." *Astronomy & Astrophysics* 399, no. 3 (2003): 1109-1114.
 4. Burwitz, V., V. E. Zavlin, R. Neuhäuser, P. Predehl, J. Trümper, and A. C. Brinkman. "The Chandra LETGS high resolution X-ray spectrum of the isolated neutron star RX J1856. 5-3754." *Astronomy & Astrophysics* 379, no. 2 (2001): L35-L38.
 5. Xu, R. X., G. J. Qiao, and Bing Zhang. "PSR 0943+ 10: A bare strange star?." *The Astrophysical Journal Letters* 522, no. 2 (1999): L109.
 6. Lyne, Andrew, George Hobbs, Michael Kramer, Ingrid Stairs, and Ben Stappers. "Switched magnetospheric regulation of pulsar spin-down." *Science* 329, no. 5990 (2010): 408-412.
 7. Alford, Mark, Matt Braby, Mark Paris, and Sanjay Reddy. "Hybrid stars that masquerade as neutron stars." *The Astrophysical Journal* 629, no. 2 (2005): 969.
 8. Jin, Zhi-Ping, Kenta Hotokezaka, Xiang Li, Masaomi Tanaka, Paolo D'Avanzo, Yi-Zhong Fan, Stefano Covino, Da-Ming Wei, and Tsvi Piran. "The Macronova in GRB 050709 and the GRB-macronova connection." *Nature Communications* 7, no. 1 (2016): 12898.
 9. Von Kienlin, A., Péter Veres, O. J. Roberts, R. Hamburg, E. Bissaldi, M. S. Briggs, E. Burns et al. "Fermi-GBM GRBs with characteristics similar to GRB 170817A." *The Astrophysical Journal* 876, no. 1 (2019): 89.
 10. Ajello, M., M. Arimoto, Magnus Axelsson, L. Baldini, G. Barbiellini, D. Bastieri, R. Bellazzini et al. "A decade of gamma-ray bursts observed by Fermi-LAT: the second GRB catalog." *The Astrophysical Journal* 878, no. 1 (2019): 52.
 11. Metzger, Brian D. "Kilonovae." *Living reviews in relativity* 20, no. 1 (2017): 3.
 12. Raaijmakers, Geert, Samaya Nissanke, Francois Foucart, Mansi M. Kasliwal, Mattia Bulla, Rodrigo Fernández, Amelia Henkel et al. "The challenges ahead for multimessenger analyses of gravitational waves and kilonova: a case study on GW190425." *The Astrophysical Journal* 922, no. 2 (2021): 269.
 13. Olausen, S. A., and V. M. Kaspi. "The McGill magnetar catalog." *The Astrophysical Journal Supplement Series* 212, no. 1 (2014): 6.

-
14. Gavriil, Fotis P., Victoria M. Kaspi, and Peter M. Woods. "A comprehensive study of the X-ray bursts from the magnetar candidate 1E 2259+ 586." *The Astrophysical Journal* 607, no. 2 (2004): 959.
 15. Astashenok, Artyom V., Salvatore Capozziello, Sergei D. Odintsov, and Vasilis K. Oikonomou. "Extended gravity description for the GW190814 supermassive neutron star." *Physics Letters B* 811 (2020): 135910.
 16. Liu, Bin, and Dong Lai. "Hierarchical black hole mergers in multiple systems: constrain the formation of GW190412-, GW190814-, and GW190521-like events." *Monthly Notices of the Royal Astronomical Society* 502, no. 2 (2021): 2049-2064.
 17. Annala, Eemeli, Tyler Gorda, Joonas Hirvonen, Oleg Komoltsev, Alekski Kurkela, Joonas Nättilä, and Alekski Vuorinen. "Strongly interacting matter exhibits deconfined behavior in massive neutron stars." *Nature Communications* 14, no. 1 (2023): 8451.
 18. Heinz, Ulrich. "From SPS to RHIC: Breaking the barrier to the quark-gluon plasma." In *AIP Conference Proceedings*, vol. 602, no. 1, pp. 281-292. AIP, 2001.
 19. Emerick, A., X. Zhao, and R. Rapp. "Bottomonia in the quark-gluon plasma and their production at RHIC and LHC." *The European Physical Journal A* 48, no. 5 (2012): 72.
 20. Teaney, D., J. Lauret, and Edward V. Shuryak. "Flow at the SPS and RHIC as a quark-gluon plasma signature." *Physical Review Letters* 86, no. 21 (2001): 4783.
 21. Arsene, I., I. G. Bearden, D. Beavis, C. Besliu, B. Budick, H. Bøggild, C. Chasman et al. "Quark-gluon plasma and color glass condensate at RHIC? The perspective from the BRAHMS experiment." *Nuclear Physics A* 757, no. 1-2 (2005): 1-27.
 22. Florkowski, Wojciech, Amaresh Jaiswal, Ewa Maksymiuk, Radoslaw Ryblewski, and Michael Strickland. "Relativistic quantum transport coefficients for second-order viscous hydrodynamics." *Physical Review C* 91, no. 5 (2015): 054907.
 23. Heinz, Ulrich, Chun Shen, and Huichao Song. "The viscosity of quark-gluon plasma at RHIC and the LHC." In *AIP Conference Proceedings*, vol. 1441, no. 1, pp. 766-770. AIP, 2012.
 24. Moore, Guy D., and Omid Saremi. "Bulk viscosity and spectral functions in QCD." *Journal of High Energy Physics* 2008, no. 09 (2008): 015.
 25. Miller, J. M., A. C. Fabian, R. Wijnands, C. S. Reynolds, M. Ehle, M. J. Freyberg, M. Van Der Klis, W. H. G. Lewin, C. Sanchez-Fernandez, and A. J. Castro-Tirado. "Evidence of Spin and Energy Extraction in a Galactic Black Hole Candidate: The XMM-Newton/EPIC-pn Spectrum of XTE J1650–500." *The Astrophysical Journal Letters* 570, no. 2 (2002): L69.
 26. Dey, Mira, Ignazio Bombaci, Jishnu Dey, Subharthi Ray, and B. C. Samanta. "Strange stars with realistic quark vector interaction and phenomenological density-dependent scalar potential." *Physics Letters B* 438, no. 1-2 (1998): 123-128.
 27. Dolan, Louise, and Roman Jackiw. "Symmetry behavior at finite temperature." *Physical Review D* 9, no. 12 (1974): 3320.
 28. Ray, Subharthi, Jishnu Dey, and Mira Dey. "Density dependent strong coupling constant of QCD derived from compact star data." *Modern Physics Letters A* 15, no. 20 (2000): 1301-1306.
 29. Gendreau, Keith C., Zaven Arzoumanian, and Takashi Okajima. "The Neutron star Interior Composition Explorer (NICER): an Explorer mission of opportunity for soft x-ray timing spectroscopy." In *Space Telescopes and Instrumentation 2012: Ultraviolet to Gamma Ray*, vol. 8443, pp. 322-329. SPIE, 2012.
 30. Vinciguerra, Serena, Tuomo Salmi, Anna L. Watts, Devarshi Choudhury, Thomas E. Riley, Paul S. Ray, Slavko Bogdanov et al. "An Updated Mass–Radius Analysis of the 2017–2018 NICER Data Set of PSR J0030+ 0451." *The Astrophysical Journal* 961, no. 1 (2024): 62.

-
31. Johnson, Kenneth. "The MIT bag model." *Acta Phys. Pol. B* 6, no. 12 (1975): 8.
 32. Weber, Fridolin. "Strange quark matter and compact stars." *Progress in Particle and Nuclear Physics* 54, no. 1 (2005): 193-288.
 33. Alford, Mark, Krishna Rajagopal, and Frank Wilczek. "Color-flavor locking and chiral symmetry breaking in high density QCD." *Nuclear Physics B* 537, no. 1-3 (1999): 443-458.
 34. Rajagopal, Krishna, and Frank Wilczek. "Enforced electrical neutrality of the color-flavor locked phase." *Physical Review Letters* 86, no. 16 (2001): 3492.
 35. Alford, Mark G., Andreas Schmitt, Krishna Rajagopal, and Thomas Schäfer. "Color superconductivity in dense quark matter." *Reviews of Modern Physics* 80, no. 4 (2008): 1455.
 36. Alford, Mark, and Sanjay Reddy. "Compact stars with color superconducting quark matter." *Physical Review D* 67, no. 7 (2003): 074024.
 37. Baldo, Marcello, M. Buballa, G. F. Burgio, F. Neumann, M. Oertel, and H-J. Schulze. "Neutron stars and the transition to color superconducting quark matter." *Physics Letters B* 562, no. 3-4 (2003): 153-160.
 38. Lawley, S., Wolfgang Bentz, and Anthony William Thomas. "Nucleons, nuclear matter and quark matter: A unified NJL approach." *Journal of Physics G: Nuclear and Particle Physics* 32, no. 5 (2006): 667.
 39. Baym, G., and S. A. Chin. "Can a neutron star be a giant MIT bag?." *Physics Letters B* 62, no. 2 (1976): 241-244.
 40. Källman, Carl-G. "Mean-field QCD model for hot/dense matter." *Physics Letters B* 134, no. 5 (1984): 363-367.
 41. Adler, Stephen L. "Generalized bag models as mean-field approximations to QCD." *Physics Letters B* 110, no. 3-4 (1982): 302-306.
 42. McLerran, Larry, and Sanjay Reddy. "Quarkyonic matter and neutron stars." *Physical review letters* 122, no. 12 (2019): 122701.
 43. Zhao, Tianqi, and James M. Lattimer. "Quarkyonic matter equation of state in beta-equilibrium." *Physical Review D* 102, no. 2 (2020): 023021.
 44. Fodor, Zoltán, and Sandor D. Katz. "A new method to study lattice QCD at finite temperature and chemical potential." *Physics Letters B* 534, no. 1-4 (2002): 87-92.
 45. Glendenning, N. K., and F. Weber. "Nuclear solid crust on rotating strange quark stars." (1992).
 46. Owen, Benjamin J. "Maximum elastic deformations of compact stars with exotic equations of state." *Physical Review Letters* 95, no. 21 (2005): 211101.
 47. Sharma, R., and S. Mukherjee. "Compact stars: a core-envelope model." *Modern physics letters A* 17, no. 38 (2002): 2535-2544.
 48. Ng, C. Y., K. S. Cheng, and M. C. Chu. "Cooling properties of Cloudy Bag strange stars." *Astroparticle Physics* 19, no. 1 (2003): 171-192.
 49. Latifah, S., Anto Sulaksono, and Terry Mart. "Bosons star at finite temperature." *Physical Review D* 90, no. 12 (2014): 127501.
 50. Andrew, Keith, Kristopher Andrew, Rebecca Brown, Benjamin Thornberry, Seth Harper, Eric Steinfelds, and Thad Roberts. "A QCD Model of the Chemical Potential Kaon Boundary Formation for a Compact Quark Star." *Bulletin of the American Physical Society* 61 (2016).
 51. Thorsson, Vestein, Madappa Prakash, and James M. Lattimer. "Composition, structure and evolution of neutron stars with kaon condensates." *Nuclear Physics A* 572, no. 3-4 (1994): 693-731.

-
52. Alford, Mark. "Color-superconducting quark matter." *Annual Review of Nuclear and Particle Science* 51, no. 1 (2001): 131-160.
53. Andrew, Keith, Eric Steinfelds, and Kristopher Andrew. "QCD Color Vector Potential Effects on Color Flavor Locked Quark Stellar Cores." *Bulletin of the American Physical Society* (2018).
54. Alford, Mark, Jeffrey A. Bowers, and Krishna Rajagopal. "Crystalline color superconductivity." *Physical Review D* 63, no. 7 (2001): 074016.
55. Casalbuoni, Roberto, Raoul Gatto, M. Mannarelli, and G. Nardulli. "Effective field theory for the crystalline colour superconductive phase of QCD." *Physics Letters B* 511, no. 2-4 (2001): 218-228.
56. Andrew, Keith, Rebecca Brown, Kristopher Andrew, Benjamin Thornberry, Seth Harper, Eric Steinfelds, and Thad Roberts. "Analysis of Mass and Radius Sensitivity of a Crystalline Quark Star to a Strong Repulsive Equation of State." *Bulletin of the American Physical Society* 61 (2016).
57. Berbel Palomeque, Marina. "On nonconvex special relativistic hydrodynamics." (2023), Thesis, Universitat Autònoma de Barcelona.
58. Marquina, Antonio, Susana Serna, and Jose M. Ibanez. "Capturing composite waves in non-convex special relativistic hydrodynamics." *Journal of Scientific Computing* 81 (2019): 2132-2161.
59. Duez, Matthew D., Yuk Tung Liu, Stuart L. Shapiro, and Branson C. Stephens. "General relativistic hydrodynamics with viscosity: Contraction, catastrophic collapse, and disk formation in hypermassive neutron stars." *Physical Review D* 69, no. 10 (2004): 104030.
60. See National Technical Information Service Document No. PB 032189 H. A. Bethe, "The theory of shock waves for an arbitrary equation of state," Office of Scientific Research and Development Paper No. 545, 1942. Copies may be ordered from the National Technical Information Service, Springfield, VA.
61. Y. B. Zel'dovich, *Theory of Shock Waves and Introduction to Gas Dynamics* Izdatel'stvo Akademii Nauk SSSR, Moscow, 1946
62. P. A. Thompson, "A fundamental derivative in gasdynamics," *Phys. Fluids* 14, 1843 1971.
63. Aloy, Miguel A., José M. Ibáñez, Nicolas Sanchis-Gual, Martin Obergaulinger, Jose A. Font, Susana Serna, and Antonio Marquina. "Neutron star collapse and gravitational waves with a non-convex equation of state." *Monthly Notices of the Royal Astronomical Society* 484, no. 4 (2019): 4980-5008.
64. Riviaccio, Giuseppe, Davide Guerra, Milton Ruiz, and José A. Font. "Gravitational-wave imprints of nonconvex dynamics in binary neutron star mergers." *Physical Review D* 109, no. 6 (2024): 064032.
65. Most, Elias R., L. Jens Papenfort, Veronica Dexheimer, Matthias Hanauske, Horst Stoecker, and Luciano Rezzolla. "On the deconfinement phase transition in neutron-star mergers." *The European Physical Journal A* 56 (2020): 1-11.
66. Sarkar, Nachiketa, and Premomoy Ghosh. "van der Waals hadron resonance gas and QCD phase diagram." *Physical Review C* 98, no. 1 (2018): 014907.
67. Vovchenko, Volodymyr, Mark I. Gorenstein, and Horst Stoecker. "van der Waals interactions in hadron resonance gas: from nuclear matter to lattice QCD." *Physical review letters* 118, no. 18 (2017): 182301.

-
68. Rodrigues, E. H., M. Dutra, and O. Lourenço. "Recent astrophysical observations reproduced by a short-range correlated van der Waals-type model?." *Monthly Notices of the Royal Astronomical Society* 523, no. 4 (2023): 4859-4868.
69. Andrew, Keith, Eric V. Steinfelds, and Kristopher A. Andrew. "The van der Waals Hexaquark Chemical Potential in Dense Stellar Matter." *Particles* 6, no. 2 (2023): 556-567.
70. Lugones, G., and Ana Gabriela Grunfeld. "Excluded volume effects in the quark-mass density-dependent model: Implications for the equation of state and compact star structure." *Physical Review D* 109, no. 6 (2024): 063025.
71. Sen, Srimoyee, and Lars Sivertsen. "Mass and radius relations of quarkyonic stars using an excluded-volume model." *The Astrophysical Journal* 915, no. 2 (2021): 109.
72. Sarkar, Nachiketa, and Premomoy Ghosh. "van der Waals hadron resonance gas and QCD phase diagram." *Physical Review C* 98, no. 1 (2018): 014907.
73. Poberezhnyuk, Roman V., Horst Stoecker, and Volodymyr Vovchenko. "Quarkyonic matter with quantum van der Waals theory." *Physical Review C* 108, no. 4 (2023): 045202.
74. Thirukkanesh, S., and F. C. Ragel. "Anisotropic compact sphere with Van der Waals equation of state." *Astrophysics and Space Science* 354 (2014): 415-420.
75. Vovchenko, Volodymyr, Anton Motornenko, Paolo Alba, Mark I. Gorenstein, Leonid M. Satarov, and Horst Stoecker. "Multicomponent van der Waals equation of state: Applications in nuclear and hadronic physics." *Physical Review C* 96, no. 4 (2017): 045202.
76. Mardan, S. A., A. Khalid, Rubab Manzoor, and Muhammad Bilal Riaz. "Anisotropic model observing pulsars from Neutron Star Interior Composition with modified Van der Waals equation of state." *The European Physical Journal C* 84, no. 10 (2024): 1018.
77. Lourenço, O., M. Dutra, C. H. Lenzi, M. Bhuyan, S. K. Biswal, and B. M. Santos. "A density-dependent van der waals model under the gw170817 constraint." *The Astrophysical Journal* 882, no. 1 (2019): 67.
78. Dutra, M., B. M. Santos, and O. Lourenço. "Constraints and correlations of nuclear matter parameters from a density-dependent van der Waals model." *Journal of Physics G: Nuclear and Particle Physics* 47, no. 3 (2020): 035101.
79. Malaver, Manuel, and Hamed Daei Kasmaei. "Analytical models for quark stars with van der Waals modified equation of state." *International Journal of Astrophysics and Space Science* 7, no. 5 (2019): 58.
80. Errehymy, Abdelghani, G. Mustafa, Youssef Khedif, Mohammed Daoud, H. I. Alrebdi, and Abdel-Haleem Abdel-Aty. "Self-gravitating anisotropic model in general relativity under modified Van der Waals equation of state: a stable configuration." *The European Physical Journal C* 82, no. 5 (2022): 1-11.
81. Poberezhnyuk, R. V., Volodymyr Vovchenko, Mark I. Gorenstein, and Horst Stoecker. "Noncongruent phase transitions in strongly interacting matter within the quantum van der Waals model." *Physical Review C* 99, no. 2 (2019): 024907.
82. Moss, Tripp, Roman Poberezhniuk, and Volodymyr Vovchenko. "Quantum van der Waals quarkyonic matter at non-zero isospin asymmetry." *arXiv preprint arXiv:2411.11996* (2024).
83. Vovchenko, Volodymyr, Anton Motornenko, Paolo Alba, Mark I. Gorenstein, Leonid M. Satarov, and Horst Stoecker. "Multicomponent van der Waals equation of state: Applications in nuclear and hadronic physics." *Physical Review C* 96, no. 4 (2017): 045202.
84. Guardone, A. L. B. E. R. T. O., and Luigi Vigevano. "Roe linearization for the van der Waals gas." *Journal of Computational Physics* 175, no. 1 (2002): 50-78.

-
85. Ibáñez, José-María, Isabel Cordero-Carrión, Miguel-Ángel Aloy, José-María Martí, and Juan-Antonio Miralles. "On the convexity of relativistic ideal magnetohydrodynamics." *Classical and Quantum Gravity* 32, no. 9 (2015): 095007.
 86. Kapusta, Joseph, Mayank Singh, and Thomas Welle. "Spinodal decomposition in Bjorken flow." *arXiv preprint arXiv:2409.16525* (2024).
 87. Fraga, Eduardo S., Alekski Kurkela, and Alekski Vuorinen. "Interacting quark matter equation of state for compact stars." *The Astrophysical Journal Letters* 781, no. 2 (2014): L25.
 88. Li, Hua, Xin-Lian Luo, and Hong-Shi Zong. "Bag model and quark star." *Physical Review D—Particles, Fields, Gravitation, and Cosmology* 82, no. 6 (2010): 065017.
 89. Huovinen, Pasi, and Péter Petreczky. "QCD equation of state and hadron resonance gas." *Nuclear Physics A* 837, no. 1-2 (2010): 26-53.
 90. Kojo, Toru, Philip D. Powell, Yifan Song, and Gordon Baym. "Phenomenological QCD equation of state for massive neutron stars." *Physical Review D* 91, no. 4 (2015): 045003.
 91. Orsaria, M., H. Rodrigues, Fridolin Weber, and G. A. Contrera. "Quark deconfinement in high-mass neutron stars." *Physical Review C* 89, no. 1 (2014): 015806.
 92. Bazavov, Alexei, Tanmoy Bhattacharya, Carleton DeTar, H-T. Ding, Steven Gottlieb, Rajan Gupta, P. Hegde et al. "Equation of state in (2+ 1)-flavor QCD." *Physical Review D* 90, no. 9 (2014): 094503.
 93. Laermann, Edwin. "The equation of state from lattice QCD." *Acta Physica Polonica. Series B, Proceedings Supplement* 3, no. 3 (2010): 611-620.
 94. Jain, Tamanna. "Analytic Modelling of Gravitational-Wave Source in General Relativity and Alternative Theories of Gravity." PhD diss., 2024.
 95. Martynov, Denis V., E. D. Hall, B. P. Abbott, R. Abbott, T. D. Abbott, C. Adams, R. X. Adhikari et al. "Sensitivity of the Advanced LIGO detectors at the beginning of gravitational wave astronomy." *Physical Review D* 93, no. 11 (2016): 112004.
 96. Aasi, J., J. Abadie, B. P. Abbott, R. Abbott, T. D. Abbott, M. Abernathy, T. Accadia et al. "The characterization of Virgo data and its impact on gravitational-wave searches." *Classical and Quantum Gravity* 29, no. 15 (2012): 155002.
 97. KAGRA Collaboration, "KAGRA: 2.5 generation interferometric gravitational wave detector." *Nature Astronomy* 3, no. 1 (2019): 35-40.
 98. Punturo, M., M. Abernathy, Fausto Acernese, B. Allen, Nils Andersson, K. Arun, Fabrizio Barone et al. "The Einstein Telescope: A third-generation gravitational wave observatory." *Classical and Quantum Gravity* 27, no. 19 (2010): 194002.
 99. Cutler, Curt. "Angular resolution of the LISA gravitational wave detector." *Physical Review D* 57, no. 12 (1998): 7089.
 100. Posselt, B., and G. G. Pavlov. "The cooling of the central compact object in Cas A from 2006 to 2020." *The Astrophysical Journal* 932, no. 2 (2022): 83.